Canadian Acoustics / Acoustique Canadienne 26(2) 3-10 (1998) ***Research article / Article de recherche***

A SYNTHETIC APERTURE MATCHED FIELD APPROACH TO ACOUSTIC SOURCE LOCALIZATION IN A SHALLOW-WATER ENVIRONMENT

Garry J. Heard
Defence Research Establishment Atlantic, PO Box 1012 Dartmouth, Nova Scotia B2Y 3Z7 CA
and
Ian Schumacher
JASCO Research Ltd., #102-7143 West Saanich Rd. Brentwood Bay, BC V8M 1P7 CA

ABSTRACT

Matched field processing is a developing technique for localizing underwater acoustic sources and inverting measured acoustic fields for ocean waveguide properties. Considerable successes have been reported using this technique in deep water and, in the recent past, the technique has shown promise for localizing acoustic sources in shallow water. This paper describes an experiment conducted in the shallow water of the Western Bank near Sable Island on the eastern Canadian continental shelf. The experiment involved examining the localization performance of a small vertical array consisting of only four hydrophones and spanning approximately one-third of the water column against a relatively low signal-to-noise ratio source in a weakly range-dependent environment. In this experiment, the source emitted a series of low-frequency tones that were detectable by Fourier analysis of the received time-series. By estimating the phase of the received signal as a function of time, it was possible to estimate the relative change in the target range during an interval. Using a modified Bartlett matched field processor, the phase information was incorporated to estimate the true target range and depth during the same interval. The results of this experiment indicate that matched field localization can be dramatically improved by incorporating auxiliary information, such as the estimated signal phase history. In this case, the performance of the vertical receiving array approximates the expected performance of a planar array with the same vertical dimension as the actual receiver and a horizontal dimension controlled by the duration of the interval during which the phase history is estimated.

SOMMAIRE

Le traitement de champs appariés est une technique en cours de développement pour localiser des sources acoustiques et inverser les champs acoustiques mesurés afin de déterminer les propriétés de guides d'ondes. On signale que cette technique a eu beaucoup de succès en eau profonde et, dernièrement, elle a eu des résultats prometteurs pour localiser des sources acoustiques en eau peu profonde. Ce rapport décrit une expérience menée lors de l'essai dans les eaux peu profondes du Banc ouest près de l'Île de Sable sur le plateau continental du Canada. Cette expérience consistait à examiner les performances de localisation d'une antenne verticale ne comprenant que quatre hydrophones et couvrant environ le tiers de la colonne d'eau vis à vis d'une cible à rapport signal/bruit relativement faible dans un environment dépendant dans une faible mesure de la distance. Lors de cette expérience, la cible émettait une série de tonalités basse fréquence détectables par analyse de Fourier de la série chronologique reçue. En estimant la phase du signal reçu en fonction du temps, on a pu estimer la variation relative de la distance de la cible pendant un intervalle donné. En utilisant un processeur de champs appariés de Bartlett modifié, on a incorporé l'information de phase pour estimer la distance et la profondeur absolues de la cible pendant le même intervalle. Les résultats de cette expérience indiquent que la localisation par champs appariés peut être grandement améliorée si l'on incorpore de l'information auxiliaire telle que la discordance de phase du signal. Dans ce cas, les performances de l'antenne verticale s'approchent de celles attendues d'un antenne planaire ayant le même dimension verticale que le récepteur en cause et une dimension horizontale déterminée par l'intervalle pendant lequel on estime la discordance de phase.

1 INTRODUCTION

The main objective of the work described in this paper was to investigate the use of a matched field processing (MFP) source localization technique with data obtained using a small vertical line array (VLA) receiver in shallow water where source motion is used to improve the resulting estimate of the acoustic source location.

Matched field processing involves optimizing the agreement between measured and modelled acoustic field values, where the modelled values are dependent on parameters such as source location that are initially unknown. A search for the unknown parameters is conducted, guided by the comparison of the measured and modelled fields. Section 2 describes matched field processing basics in more detail.

This paper presents a technique for handling acoustic source motion in MFP localization when it is possible to estimate the relative motion of the source. In our example, the relative phase change of tonal signals during the observation intervals provided the required estimates of relative source motion which was not restricted to constant velocity. Other researchers have considered MFP with moving sources, notably Zala and Ozard [1] who allow for constant source motion during the observation period, and Tantum and Nolte [2] who employ source dynamics in a new processor to improve tracking capabilities over an extended period of observation. Our technique could be extended to include a search over a completely unknown or partially known track, but this would greatly increase the processing demands on the method. In essence, the advantage of using spatially coherent processing techniques over incoherent methods is demonstrated in this work.

Using experimental data, an illustration of the MFP performance enhancement with the inclusion of temporal field information is given. One interpretation of this enhanced performance is that the inclusion of the temporal information allows the VLA to function as a virtual planar array with a vertical dimension equal to the vertical extent of the VLA and a horizontal dimension controlled by the extent of the radial source motion during the integration period. This paper illustrates the gains to be had from spatially coherent processing. It is also possible to achieve improvement by processing across multiple frequencies in a coherent fashion [3].

In the following section, the concepts of MFP and the standard Bartlett processor are introduced. Section 3 describes the field trial and experimental setup. Section 4 provides details of the trial area environment and the propagation model used in the MFP. Section 5 describes the modification of the Bartlett processor to include temporal field information. Section 6 describes how phase tracking was used to include the temporal information in the data obtained from the field trial. Section 7 shows how the MFP performance improves with the inclusion of successively longer data samples. Section 8 shows how the acoustic source can be tracked over an extended period of time. Finally, Section 9 summarizes the results of this work.

2 MATCHED FIELD PROCESSING

Matched field processing is the term applied to an acoustic source localization technique, generally attributed to Bucker [4], that attempts to optimize the correlation between a set of measured field values and a replica set generated by assuming a source location and employing an acoustic propagation model. An excellent introduction to the topic was written by Tolstoy [5]. Recently, in addition to localization, MFP has been applied to geoacoustic inversion and also to ocean tom-

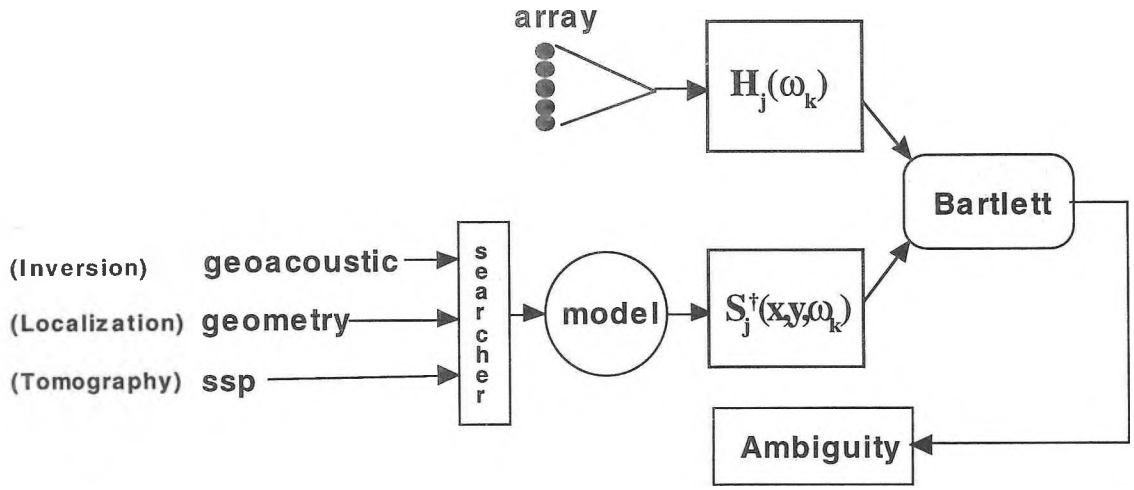

Figure 1 Block diagram of a straight-forward MFP scheme employing a Bartlett processor. By searching over different parameters MFP can be employed for various purposes, such as: inversion, localization, or tomography.

ography.

Figure 1 shows a block diagram of a typical MFP scheme. Field samples are measured by hydrophones in an array and a data sample taken over a short time interval, hereafter referred to as a 'snapshot', is Fourier transformed and a cross-spectral matrix (CSM) for one or more frequency bins is created. The measured CSM is then correlated with a set of steering vectors generated by assuming a suitable set of inputs to an acoustic propagation model. In this case, the suitable model inputs are the sound-speed profile, geoacoustic properties of the bottom, the bathymetry, and a guessed location for the source. In Figure 1 the correlation is carried out by a Bartlett correlator, to be described later. It is common to call the correlation function, the processor. Usually, the assumed source location (or whatever parameters are unknown) are varied in a systematic fashion by the searcher block and the correlation is computed for each input state. The correlation is normalized so that a maximum of unity is obtained when the measured and modelled fields are proportional and zero is obtained when the fields are completely uncorrelated. In this fashion, the maxima of the correlation are interpreted as occurring at best estimates of the unknown parameter values.

Rarely is the environment sufficiently well known in MFP problems that significant correlation results from the input of first-estimate values for the source-receiver geometry and geoacoustic parameters. Usually, it is necessary to perform a search over at least some parameter intervals, particularly for the receiving hydrophone locations, in order to obtain a significant correlation at the true source location. Collins and Kuperman [6] call this combined search for source position and environmental parameters 'focalization'. In the case of the trial data analyzed here, the model parameters were known sufficiently well that an indication of the true source location was obtained directly from the correlation values with estimated environmental inputs; however, the correlation at the true location was not the largest value obtained, and so, without *a priori* knowledge we would have misidentified the source location. In order to assess just the effect of the inclusion of the temporal information, we froze the environmental parameters and searched only over the location parameters.

The Bartlett processor is the most often used matched field processor and is a simple normalized correlation of the measured and modelled acoustic fields. With an extension for an incoherent sum over multiple frequencies, ω_k, we can write the Bartlett processor as

$$A(x,y) = \frac{\sum_{k=1}^{K} \left| \sum_{j=1}^{N} H_j(\omega_k) S_j^{\dagger}(x,y,\omega_k) \right|^2}{\sum_{k=1}^{K} \sum_{j=1}^{N} |H_j(\omega_k)|^2 \sum_{k=1}^{K} \sum_{j=1}^{N} |S_j(x,y,\omega_k)|^2}, \qquad \text{Eq. 1}$$

where $H_j(\omega_k)$ is the field measured on hydrophone j at frequency k, $S_j(x,y,\omega_k)$ is the modelled field for hydrophone j and frequency k with the source at location (x,y), and † denotes the complex conjugate. H_j may be obtained from each hydrophone by Fourier transformation of a data snapshot of a length determined empirically and partially dictated by the source's range-rate and the range-dependence of the environment. The S_j are obtained directly from a model run. This processor will be modified in Section 5 to include multiple snapshots from a moving source.

3 THE FIELD TRIAL

In July 1994, Defence Research Establishment Atlantic (DREA) conducted a shallow-water MFP experiment on the Western Bank area of the Scotian Shelf. The MFP experiment employed the DREA OMEGA Vertical Line Array (VLA) [7] as a receiver. At the time, only 4 stations of this modular array were available for use. These four hydrophone stations were located at depths 43.8, 51.0, 58.2, and 72.5 metres providing an aperture of just 28.7 m, which represented less than one-third of the nominal 95 m water depth. The array was assumed to be vertical during the data collection. The VLA was not outfitted with tilt sensors, but the arrival times of impulsive acoustic signals were consistent with less than one degree of tilt.

The matched field experiment involved towing the DREA Moving Coil Projector (MCP) [8] at a nominal depth of 30.5 m along a straight path approximately 12 km in length past the location of the VLA. The MCP simultaneously emitted three tones at 17, 21.5, and 30 Hz. The received signal-to-noise ratio (SNR) for these tones varied during the trial from 6 to 9 dB in a 1-Hz wide band. In MFP studies currently published, SNR values are typically much higher than our current levels. This is not to say that MFP requires a high SNR, it just means that the ever present effects of mismatch are more easily overcome with a strong signal. In the current work, the available SNR was more than sufficient.

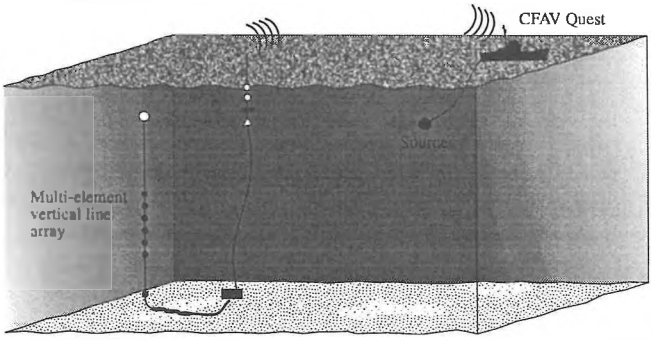

Figure 2 Experiment setup for the VLA matched field experiment.

Figure 2 shows the experimental setup for the MFP experiment. Note that the location of the VLA is not exactly the same as the location of the surface telemetry float. The horizontal distance between the VLA and the surface float is as much as several hundred metres (~2 cables) and the orientation and range change from deployment to deployment and at the mercy of current, wind, and wave conditions. This uncertainty in the receiver position was of considerable importance to the MFP analysis. In contrast, the position of the acoustic source is relatively accurately known due to the measurement of the cable scope, MCP depth, and global positioning system (GPS) navigation. Since the receiver positions are less accurately known than the source position, we decided to initially localize the receiver rather than the source (as is more commonly done). The bottom hydrophone location was used as a reference position. Later, when a reasonably accurate receiver position had been estimated, we reversed the procedure and localized the source.

4 THE ENVIRONMENT

The trial site chosen for this experiment was near the edge of the continental shelf. A bathymetric survey was conducted and it was determined that along the tow direction, which was almost parallel to the shelf edge, the mean bottom slope locally was approximately 0.08°; however, the variance in the depth is large compared to the mean and range-independent modelling was deemed appropriate only for a 4-km long portion of the tow to the east of the array position. Thomson's finite-difference parabolic equation model (PE) [9] was used to model the range-independent portion of the track. To the west of the array, an adiabatic normal mode approximation was used in the modelling to reduce the effects of mismatch in the bathymetry by including a smoothed version of the estimated bathymetry. This time, the KRAKEN model of Porter [10] was used, because the model is well suited to the adiabatic approximation and the numerical techniques that were employed. Run times were also significantly less with this approach rather than the alternative of recomputing the PE field estimate a number of times. Perpendicular to the tow path the bathymetry exhibits a mean slope about twice that along the tow-path direction. Although this cross-slope will have some effect on the propagation, no account of it was included in the modelling since the impact was expected to be small.

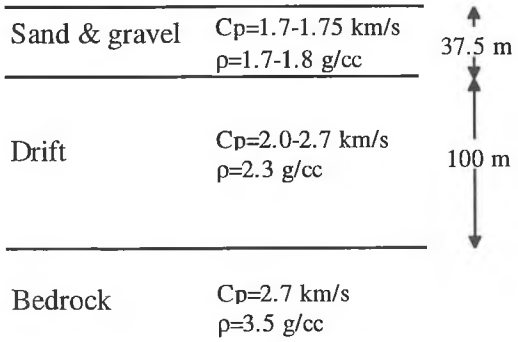

Figure 3 Geoacoustic model used.

Sound-speed profiles were collected with the aid of expendable bathythermographs (XBT) throughout the duration of the field trial. Thermal data were converted to sound speed by assuming a constant 35 parts per million salinity concentration and using Medwin's [11] empirical formula. Over a three-day period, eleven XBT profiles were acquired in an 11 km by 24 km area enclosing the MFP tow-path. These profiles showed considerable similarity in the first 100 m of depth (note that the maximum depths varied from 80 to 250 m, depending on location) and so an average sound-speed profile was used for the MFP localization. In retrospect, using the average profile may have contributed to the mismatch, since there is an indication of an east-west variation in the sound-speed profile that probably should have been included in the optimization. Typically, we obtained maximum correlations between the measured and modelled fields in the range 0.6 to 0.8 indicating a probable match between the model environment and the actual environment, but still with some room for improvement. The extent of the mismatch produced by employing the averaged profile has not been examined, but it could be a significant factor in the remaining error.

The geoacoustic properties of the area were taken mostly from a report by Osler [12] that summarizes the information available for the experiment site. Since this work was done, some additional estimates of the sub-surface structure have become available and it is known that some of the geoacoustic data was misinterpreted. Specifically, the layer of Scotian Shelf Drift (sand, clay and silt, pebbles, cobbles and boulders) included beneath the uppermost sediment layer of relatively hard sand and gravel is absent in the region where the experiment was carried out. Seismic soundings in the area have shown that the sand lies directly over bedrock [13] and that there is no recognizable layer of Drift. Fortunately, the highly reflective sand layer appears to have reduced the importance of the error in our geoacoustic model and good localization results were obtained. Figure 3 shows the geoacoustic model used. Absorption parameters are not critical, and not terribly well defined; we used 0.46 dB/λ for the sand, 0.3 dB/λ for the Drift, and 0.08 dB/λ for the bedrock [12]. Modelling has also shown that the acoustic fields in the water column are not strongly dependent on the shear properties, so shear values were not generally included in the modelling. When shear was included we used 260 m/s for the sand and Drift [14], and 800 m/s for the bedrock [12].

5 ENHANCED PROCESSOR

The Bartlett processor, Eq. 1, was modified to include the effect of source motion over an extended period of time. Since Eq. 1 uses snapshots of data to estimate $H_j(\omega_k)$, an obvious extension of the processor is to combine a number of snapshots into a single estimate of the correlation. One way of combining multiple data snapshots is given below,

$$A(x,y)=\frac{\sum_{k=1}^{K}\left|\sum_{u=1}^{U}\sum_{j=1}^{N}H_j(\omega_k,t_u)S_j^{\dagger}\left(x+r_x(t_u),y+r_y(t_u),\omega_k\right)\right|^2}{\sum_{k=1}^{K}\sum_{u=1}^{U}\sum_{j=1}^{N}\left|H_j(\omega_k,t_u)\right|^2\sum_{k=1}^{K}\sum_{u=1}^{U}\sum_{j=1}^{N}\left|S_j\left(x+r_x(t_u),y+r_y(t_u),\omega_k\right)\right|^2},$$

Eq. 2

where $H_j(\omega_k,t_u)$ represents the spectral estimate for hydrophone j, at frequency ω_k, using the u^{th} data snapshot, and $S_j\left(x+r_x(t_u),y+r_y(t_u),\omega_k\right)$ represents the modelled field estimate at frequency ω_k for an assumed source position $\left(x+r_x(t_u),y+r_y(t_u)\right)$. The position (x,y) is the assumed source position at the time of the first snapshot, and r_x and r_y represent the relative motion of the source during the total interval of the U snapshots. Coordinates x and y may represent range and depth (as they do in this application), azimuth and bearing, or any other coordinates as required by the application.

Eq. 2 combines the information from the individual snapshots semi-coherently. For each snapshot, data from each hydrophone are combined in a spatially coherent sense, but contributions from different frequencies are summed incoherently. Variations of Eq. 2 have been tried, but this particular semi-coherent approach appears, qualitatively, to provide a useful combination of robustness and spatial resolution.

Direct application of Eq. 2 requires breaking an interval of data into U snapshots. In general, these snapshots may be randomly selected during the interval; however, the simplest approach is to order the snapshots chronologically. The snapshots may also overlap in time. The spacing and length of the snapshots are in part dictated by the behaviour of the source. The total length of the interval depends on the frequency stability of the emitted tones, or upon the available knowledge of the signal dynamics. Our approach has been empirical with only rough guidelines for snapshot length and overlap based on frequency and spatial resolution concerns. In our application of Eq. 2 to the trial data we have used a slightly modified form that will be described in the next section.

Successful use of Eq. 2 requires an accurate estimate of the relative motions. People immediately ask; why use Eq. 2 if you have the relative motion estimates? The answer to this question is that Eq. 2 provides an estimate of, for example absolute range and depth, when you only know the relative change in the source range and depth. With additional assumptions about source behaviour, Eq. 2 also provides depth estimates when no prior information was available. The next section shows how the relative motions were obtained for the field trial data previously discussed.

6 PHASE TRACKING

Application of Eq. 2 to the current experiment was carried out by making a reasonable assumption about the vertical source motion and by using phase tracking to estimate the relative radial source motion. Since the acoustic source was towed at nearly constant speed and weather conditions were favourable, it was assumed that the depth variations of the acoustic source during the tow were negligible: this implies that $r_y(t_u)\to 0$ for all t_u. An estimate of r_x was obtained by employing an analysis to estimate the phase of the received sinusoidal signals and interpreting the temporal change in phase to be due entirely to a change in the source-receiver separation. The remainder of this section describes in more detail the process of determining r_x.

The first step in the process of determining r_x is to heterodyne the received time-series by the known source frequency of interest. Note that in this case we knew the projector frequencies, but in general we have found that good results are obtained even when the signal frequency is initially unknown and an estimate from a spectral analysis is used. Once the signal of interest has been moved to baseband, a relatively narrow-bandwidth low-pass filter operation removes unwanted noise. The filter can be almost any linear, steep roll-off filter with parameters chosen by examining the signal spectrum near baseband. Optimal filters can also be designed based on models of the source motion [15], but in general this is not necessary. After filtering, the signal is decimated to reduce the number of samples and ease subsequent handling. The amount of decimation is controlled by the retained bandwidth of the signal, the magnitude of the derivative of the heterodyned and filtered signal with respect to time, and by the final interval at which estimates of r_x are required.

The second step in the process is to recover the phase, $\phi(t)$, of the received signal. Several methods of performing this operation are available, but our preferred method involves a numerical integration of the heterodyned, filtered, and decimated signal $g(t)=a(t)\exp(i\,\phi(t))$, where a represents the possibly time-dependent amplitude. Given the form of $g(t)$, it is easy to see that the change in the phase from time 0 to time t is given by

$$\phi(t)=\int_0^t \mathrm{Im}\left[\frac{g'(\zeta)}{g(\zeta)}\right]d\zeta,$$

Eq. 3

where the prime denotes the derivative with respect to time. The advantage of Eq. 3 is that the resulting phase does not

need to be unwrapped as $\phi \in \Re$. Other methods usually result in the phase estimate being defined on the interval $(-\pi, \pi]$ and require the additional step of unwrapping the phase estimates. Once $\phi(t)$ has been determined, then $r_x(t)$ is given by

$$r_x(t) = \frac{c}{\omega}\phi(t), \qquad \textbf{Eq. 4}$$

where ω is the radial frequency of interest and c is approximated by the phase speed of the dominant mode or ray arrival. The discrete time equivalents of Eqs. 3 & 4 are easily obtained by approximating the derivative of $g(t)$ by a first order difference. In this work, $r_x(t)$ was estimated from each of the three tonals and an average was formed for final use.

The use of the filter suggests a way to apply Eq. 2 in this particular application. The output of the filter is itself an approximation of $H_j(\omega_k, t_u)$ with the harmonic time dependence removed by the shift to baseband. This implies that we can interpret u as being only 1 sample long (although the filter will likely have an integration time of several seconds to a minute) and form the numerator of Eq. 2 by taking the dot product of the filtered data with the model output directly, without the need to add the harmonic dependence, $e^{i\omega t}$, into the model predictions (remember that the field samples do not occur at the same time). This technique saves computation time and works quite well in practice.

The discussion to this point has assumed that we are receiving a direct-path signal from the acoustic source. In practice, we usually receive a signal composed of several multi-path arrivals. The presence of the multi-path results in a bias in the estimated phase and can result in severe errors in the estimate of radial motion. The bias term is small if the direct path amplitude dominates; unfortunately this can't be counted on in practice. In our current application with a VLA in shallow water, a simple solution to the multi-path bias was to sum the signals from each hydrophone in the array thereby effectively beamforming horizontally. Alternatively, one can think of this as mode filtering. In the present case, we favour mode 0 by simply summing the hydrophone signals. Our mapping of phase-change to distance-change (Eq. 4) should therefore use the phase speed of mode 0 for c. Although we have only used the mode 0 signals in this work, the potential exists to estimate the change in distance using the contributions from each mode.

Simulation of the multi-path bias showed that it could be a considerable problem in our current application. Using the beamformed signal, rather than the hydrophone signals directly, indicated that a dramatic improvement in the radial range estimates should be possible. On comparing the radial range estimates from GPS positions with those from the phase-tracked beamformed signal, an excellent agreement was obtained.

7 SYNTHETIC APERTURE

With phase-tracking accomplished for each tonal of interest,

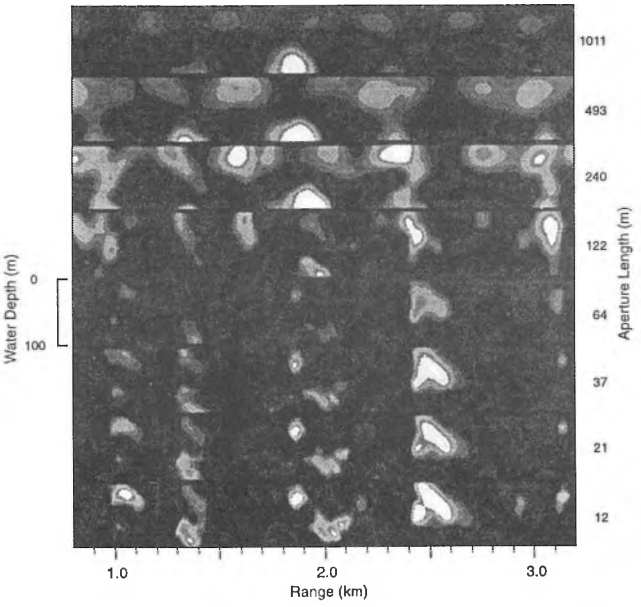

Figure 4 Array localization versus aperture length using known source location. Shortest aperture (12 m) is at bottom, longest aperture (1011 m) at top. Each ambiguity strip represents 2.4 km by 100 m. True array location estimated to be at 2 km range (±360 m) and 72.5 m depth.

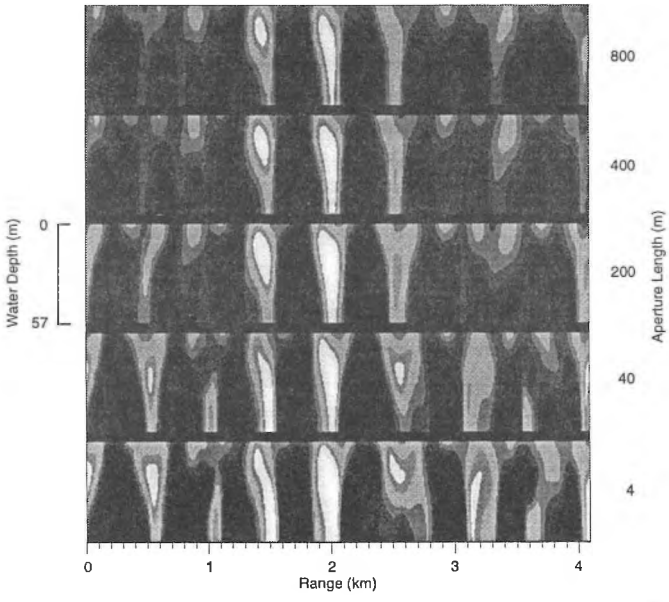

Figure 5 Source localization vs. aperture length using estimated array position. Shortest aperture (4 m) at bottom, longest aperture (800 m) at top. Each ambiguity strip represents a region 4.1 km by 57 m. True source location at 2 km range and 30 m depth.

we can now proceed to apply Eq. 2 and obtain a synthetic aperture matched field result. The aperture is equivalent to the distance travelled by the source during the interval of observation. Figure 4 shows the ambiguity surfaces obtained for 8 different aperture lengths in the region where range-independent modelling was found to be adequate. Each strip in the figure represents the depths from 0—100 m and a 2.4 km range interval. In this figure, and in all the following figures, lighter regions indicate higher correlation values. The shortest aperture is at the bottom of the figure and represents a source motion of only 12 m. This result is equivalent to a single snapshot estimate (approx. 6 seconds integration time) and the result fails to accurately localize the receiving array (in fact, we were unable to localize the source for any choice of processing parameters without employing phase tracking). For the data segment processed, the true array position was estimated to be at a range of (2±0.2) km and a depth of (72.5±1) m (relative to a point on the surface directly above the MCP at the start time of the data segment). As aperture length is increased, the number of false localizations decreases. For aperture lengths exceeding 122 m a useful localization is obtained.

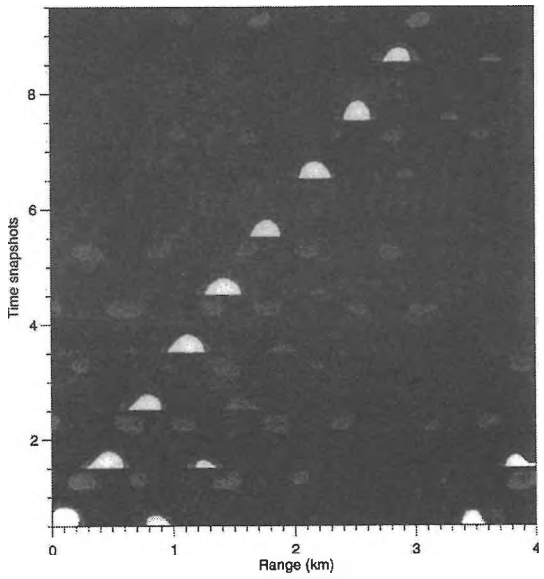

Figure 6 Tracking the array position as a function of time using known source location. Aperture length is 300 m.

Figure 5 shows the result of using the estimated location of the receiving array and applying the synthetic aperture technique to localize the source. In this figure, the aperture lengths vary from 4 to 800 m with the shortest aperture at the bottom and the longest at the top. Each strip represents a region just over 4 km long and water depths 0–57 m. The true source location is accurately localized for each aperture tried, but an improvement in the results is seen for apertures up to 200 m. For the longer apertures we see a reduction in the number and amplitude of false localizations, but we also note a reduction in the correlation value at the true location. This limitation is most likely the result of cumulative mismatch.

8 TRACKING

Target tracking can be accomplished by sequentially processing segments of data. Sequentially processing intervals of data is not an optimal way of performing tracking [2], but it does illustrate that the synthetic aperture technique can be successfully applied at any starting point in the data. Figure 6 shows

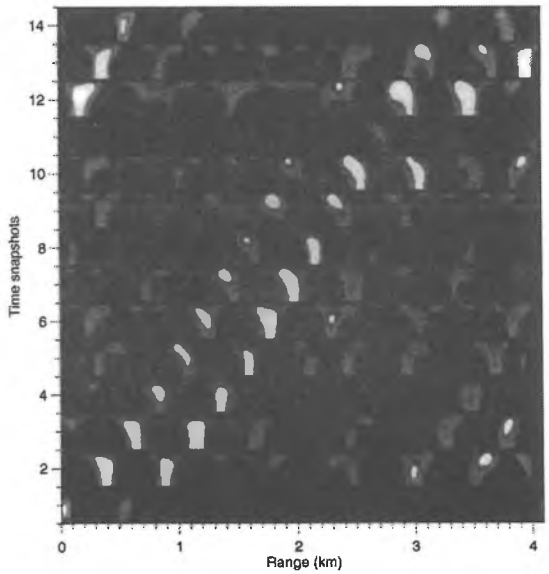

Figure 7 Tracking the source location using an estimated array location. Aperture length is 200 m.

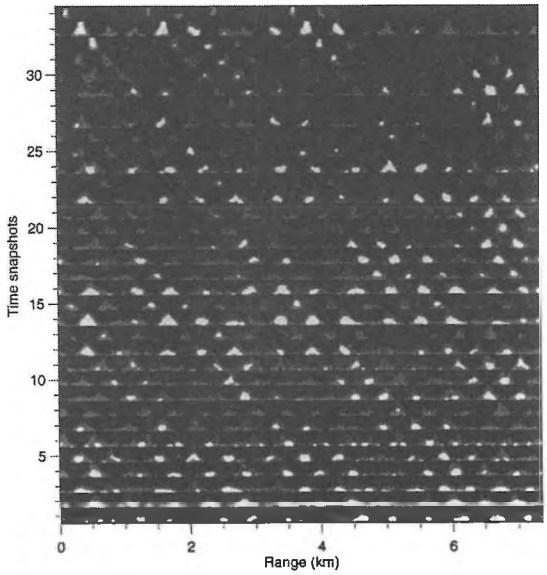

Figure 8 Source track in the range-dependent region using the assumed array location . Note the repetition of ambiguity at intervals in range.

the result of employing a 300 m aperture length to localize the receiving array. In this figure the array location is unambiguously tracked as the source is towed away from the receiver.

Figure 7 shows the result of tracking the source using the estimated receiver location. The source is ambiguously tracked from 0.5 to 3.2 km in the 14 snapshots shown. The increased ambiguity in the figure (relative to the array track shown earlier) is undoubtedly the result of increased mismatch due to using the estimated receiver location. In this situation where there is considerable ambiguity, more sophisticated tracking algorithms would likely improve the localization. Wilmut, Ozard and Yeremy [16] discuss one technique that should be applicable.

Figure 8 shows the result of tracking the source along a 7 km path in the range-dependent region west of the receiving array. Construction of this figure required using an estimated receiver location and the results show the effects of increased mismatch due to both the receiver position uncertainty and the more complicated geometry. The true source location begins in the lowest strip at just over 7-km range and ends in the top strip at approximately 0.5-km range.

9 CONCLUSIONS

By including temporal data in MFP localization, enhanced performance is realized through the use of spatially coherent processing. In this particular application, the results indicate that even a very modest VLA can be used to accurately localize a moderate level acoustic source provided that it is possible to estimate accurately the relative source motion, either through other measurements, by dynamic motion modelling, or by searching for the motion. The source motion itself can be non-uniform. The results were best where range-independent modelling was appropriate, but useful results were also obtained in an area of weak range-dependence.

As we have discovered since completing this study, significant mismatch in the geoacoustics and in the structure of the sound-speed profile were included in our modelling. Refinement of the model inputs or focalization would likely result in further enhancement of the localization performance; however, the excellent results indicate that at least for the low-grazing angles involved our assumed environment was sufficiently close enough to the real world.

The technique of phase-tracking tonal signals, while not always applicable, does when it can be applied result in an estimate of the relative change in source position. The use of suitable models or assumptions of source motion and MFP techniques can then be used to obtain absolute source range and depth estimates. The applicability of the technique has been empirically demonstrated and future work may now consider the SNR, range-rate limitations, multi-path environment, and other factors affecting the applicability of the method.

REFERENCES

1. Zala, C.A. and Ozard, J.M., 'Matched-field processing for a moving source.' J. Acoust. Soc. Am. **92**, p. 403-417, July 1992.
2. Tantum, S.L. and Nolte, L.W., 'Tracking and localizing a moving source in an uncertain shallow water environment.' J. Acoust. Soc. Am. **103**, p. 362-373, Jan. 1998.
3. Michalopoulou, Z.H. and Porter, M.B., ' Source tracking in the Hudson Canyon Experiment.' J. Computational Acoustics **4**, p. 371-383, Dec. 1996.
4. Bucker, H.P., 'Use of calculated sound fields and matched-field detection to locate sound sources in shallow water.' J. Acoust. Soc. Am., **59**, p. 368-373, Feb. 1976.
5. Tolstoy, A. *'Matched field processing for underwater acoustics.'* World Scientific, Singapore, 1993.
6. Collins, M.D. and Kuperman, W.A., 'Focalization: Environmental focusing and source localization.' J. Acoust. Soc. Am., **90**, p. 1410-1422, Sep. 1991.
7. Risley, W.C. and Bruce, A.A., 'The OMEGA acoustic research system.' Proc. Oceans '93, **II**, p. 59-64, 1993.
8. Osler, J.C. and Chapman, D.M.F., 'Source level calibration of the DREA moving coil projector.' DREA Technical Memorandum TM 95/215, May 1995.
9. Thomson, D.J., 'Wide-angle parabolic equation solutions to two range-dependent benchmark problems.' J. Acoust. Soc. Am., **87**, p. 1514-1520, Apr. 1990.
10. Porter, M., 'The KRAKEN normal mode program.' SACLANTCEN Memorandum SM-245, Sep. 1991.
11. Medwin, H., 'Speed of sound in water: A simple equation for realistic parameters.' J. Acoust. Soc. Am., **58**, p. 1318-1319, 1975.
12. Osler, J.C., 'A geo-acoustic and oceanographic description of several shallow water experimental sites on the Scotian Shelf.' DREA Technical Memorandum TM 94/216, Nov. 1994.
13. Courtney, R.C., private communication, Marine Geophysics, Geological Survey of Canada, Bedford Institute of Ocean Sciences, Dartmouth, NS, Canada.
14. Dodds, D.J., 'Sea floor sound speed estimates from wide angle reflectivity: software development.' DREA Contractors Report CR/91/403, Jan 1991.
15. Schumacher I. and Heard, G.J., 'Removal of time-varying Doppler using phase tracking with application to ocean warming measurements.' J. Acoust. Soc. Am., **96**, p. 1805-1812, Sep. 1994.
16. Wilmut, M.J., Ozard, J.M. and Yeremy, M.L., 'Tracking in range versus time with application to matched field processing of vertical line array data.' Canadian Acoustics **25**, p. 21-27, 1997.